



1 Permafrost degradation and nitrogen cycling in Arctic rivers: Insights from
2 stable nitrogen isotope studies

3 Adam Francis^{1*}, Raja S. Ganeshram¹, Robyn E. Tuerena², Robert G.M. Spencer³, Robert
4 M. Holmes⁴, Jennifer A. Rogers³, Claire Mahaffey⁵

5 ¹School of Geosciences, University of Edinburgh, Edinburgh, UK

6 ²Scottish Association for Marine Science, Oban, UK

7 ³Department of Earth, Ocean & Atmospheric Science, Florida State University, Tallahassee,
8 Florida, USA

9 ⁴Woodwell Climate Research Center, Falmouth, Massachusetts, USA

10 ⁵Department of Earth, Ocean and Ecological Sciences, University of Liverpool, UK

11 *Correspondence to: adam.francis@ed.ac.uk

12 **Abstract**

13 Across the Arctic, vast areas of permafrost are being degraded by climate change, which has the
14 potential to release substantial quantities of nutrients, including nitrogen into large Arctic rivers.
15 These rivers heavily influence the biogeochemistry of the Arctic Ocean, so it is important to
16 understand the potential changes to rivers from permafrost degradation. This study utilised
17 dissolved nitrogen species (nitrate and dissolved organic nitrogen (DON)) along with nitrogen
18 isotope values ($\delta^{15}\text{N-NO}_3^-$ and $\delta^{15}\text{N-DON}$) of samples collected from permafrost sites in the
19 Kolyma River and the six largest Arctic rivers. Large inputs of DON and nitrate with a unique
20 isotopically heavy $\delta^{15}\text{N}$ signature were documented in the Kolyma, suggesting the occurrence of
21 denitrification and highly invigorated nitrogen cycling in the Yedoma permafrost thaw zones along
22 the Kolyma. We show evidence for permafrost derived DON being recycled to nitrate as it passes
23 through the river, transferring the high ^{15}N signature to nitrate. However, the potential to observe
24 these thaw signals at the mouths of rivers depends on the spatial scale of thaw sites, permafrost
25 degradation and recycling mechanisms. In contrast with the Kolyma, with near 100% continuous
26 permafrost extent, the Ob' River, draining large areas of discontinuous and sporadic permafrost,
27 shows large seasonal changes in both nitrate and DON isotopic signatures. During winter months,
28 water percolating through peat soils records isotopically heavy denitrification signals in contrast
29 with the lighter summer values when surface flow dominates. This early year denitrification signal
30 was present to a degree in the Kolyma but the ability to relate seasonal nitrogen signals across
31 Arctic Rivers to permafrost degradation could not be shown with this study. Other large rivers in
32 the Arctic show different seasonal nitrogen trends. Based on nitrogen isotope values, the vast
33 majority of nitrogen fluxes in the Arctic rivers is from fresh DON sourced from surface runoff
34 through organic-rich top-soil and not from permafrost degradation. However, with future
35 permafrost thaw, other Arctic rivers may begin to show nitrogen trends similar to the Ob'. Our
36 study demonstrates that nitrogen inputs from permafrost thaw can be identified through nitrogen
37 isotopes, but only on small spatial scales. Overall, nitrogen isotopes show potential for revealing
38 integrated catchment wide nitrogen cycling processes.

39 **1 Introduction**

40 The Arctic Ocean contains ~1% of global ocean volume but receives greater than 10% of the total
41 global riverine discharge (Frey and McClelland, 2009). This disproportionate influence of rivers



42 means that any changes in riverine inputs will likely have significant implications on marine
43 chemical, physical and biological processes as well as in the rivers themselves (Holmes *et al.*,
44 2012a). River biogeochemistry and discharge also integrate catchment wide processes, making
45 them potentially sensitive indicators of change to the terrestrial environment (Holmes *et al.*, 2000).
46 With diminishing sea ice and opening of surface waters to light, Arctic productivity is sensitive to
47 riverine nutrient inputs and particularly nitrogen which is the limiting nutrient in coastal areas
48 (Thibodeau *et al.*, 2017).

49 Biologically available nitrogen can exist as dissolved inorganic nitrogen (DIN) in forms of nitrate,
50 nitrite and ammonium. DIN is calculated as the sum of these three forms ($DIN = NO_3^- + NO_2^- +$
51 NH_4^+) (McCrackin *et al.*, 2014). These forms can be taken up by primary producers (Tank *et al.*,
52 2012). Nitrite and ammonium are highly biologically labile and so only persist for a short time
53 before being converted into nitrate or assimilated. Nitrogen can also exist as dissolved organic
54 nitrogen (DON) but these forms generally need to be broken down (remineralised) into DIN before
55 uptake can occur (Tank *et al.*, 2012). DON is calculated as the difference between total dissolved
56 nitrogen (TDN) and DIN: ($DON = TDN - DIN$) (Frey *et al.*, 2007). Nitrate is expected to be the
57 dominant species so a simplification can be made to $DON = TDN - NO_3^-$. As part of the nitrogen
58 cycle, exchange between these pools occurs in riverine and coastal areas depending on
59 environmental conditions. In oxic conditions, assimilation and nitrification occur, while
60 denitrification can be dominant in anoxic conditions (Voigt *et al.*, 2017).

61 Extensive areas of permafrost influence most of the riverine inputs to the Arctic Ocean. Permafrost
62 is defined as '*any subsurface material that remains below 0°C for at least two consecutive years*'
63 (Zhang *et al.*, 1999). It is defined exclusively on the basis of temperature, not whether ice is present
64 (Brabets *et al.*, 2000). Permafrost can stabilise ancient soils, preventing breakdown of soil organic
65 matter and is classified based on its spatial extent and thickness. Continuous permafrost has 90-
66 100% aerial extent and is 100-800m thick, while discontinuous has 50-90% extent and is 25-100m
67 thick (Anisimov and Reneva, 2006).

68 Permafrost undergoes degradation (or thaw) through different mechanisms. The most common is
69 active layer deepening, where the top layer of soil that thaws and refreezes each year becomes
70 deeper due to increased summer temperatures and the influx of precipitation (Nelson *et al.*, 1997).
71 This increases the depth of permafrost, allowing the active layer to penetrate previously frozen soil.
72 In permafrost with a high ice content, the melting of the ground ice can cause the collapse and
73 subsidence of surrounding soil horizons, forming thermokarst terrain. Permafrost can also degrade
74 through riverbank or coastal erosion, cutting through deep horizons of permafrost promoting rapid
75 and often catastrophic degradation. These mechanisms all lead to increases in soil microbial activity
76 that release dissolved nitrogen from previously frozen organic matter. The proportion of the
77 released nitrogen species vary depending on the degradation mechanism and the degree of thawing.

78 Climate change is causing annual surface air temperatures within the Arctic to increase at almost
79 twice the rate of the global average (Hassol *et al.*, 2004). In 2010, air temperatures in the Arctic
80 were 4°C warmer than the reference period of 1968 – 1996 (NOAA, 2014). A further 4 to 7°C
81 increase is expected by the end of the century (Hassol *et al.*, 2004). These dramatic temperature
82 changes will result in the Arctic experiencing unprecedented impacts on its environments. Over the
83 whole pan-Arctic watershed, river discharge is increasing by an estimated $5.6\text{km}^3\text{y}^{-1}$ each year
84 based on observations from 1964 - 2000 (McClelland *et al.*, 2006). Discharge has already increased



85 by ~10% in Russian rivers compared to this reference period (Peterson *et al.*, 2002). Permafrost is
86 at high risk of degradation with climate change with estimates that 10% of permafrost in the
87 northern hemisphere has disappeared in the last 100 years (NSIDC, 2018). Predictions of future
88 losses vary but a recent study predicts 4.8 or 6 million km² of permafrost (32 or 40% of global total)
89 would be lost for a global temperature increase of 1.5 or 2°C respectively (UNFCCC, 2015;
90 Chadburn *et al.*, 2017).

91 Riverine biogeochemistry across the Arctic will be significantly affected by these changes due to
92 liberation of nutrients and organic matter from the degrading permafrost and alterations to nutrient
93 cycling within Arctic rivers. Although there has been considerable research into the effects of
94 permafrost thaw on organic matter and carbon fluxes (Frey and Smith, 2005; Schuur *et al.*, 2009;
95 Vonk *et al.*, 2013; Spencer *et al.*, 2015), there are fewer studies on nitrogen loading in Arctic rivers
96 and fewer still on cycling and processing. Some of the proposed dynamics of nitrogen cycling from
97 permafrost degradation have been described in a study of Alaskan permafrost by Harms *et al.*,
98 (2013). The active layer of soil is rich in fresh organic matter with a high C:N ratio. Within this
99 layer, biotic assimilation of nitrate occurs along with denitrification in anaerobic conditions. With
100 limited permafrost thaw, nitrogen export from this layer will largely be in the form of DON rather
101 than nitrate. Much of the Arctic is covered in many meters of peat so it is argued that this may apply
102 to large areas of Arctic watersheds, especially western Siberia (Frey and McClelland, 2009). As
103 watershed mean annual air temperature (MAAT) increases past the threshold limit for permafrost
104 (-2°C – catchment temperature where permafrost begins to thaw) DON concentrations in streams
105 and rivers rapidly increase, with little changes in nitrate concentrations (MacLean *et al.*, 1999; Frey
106 *et al.*, 2007).

107 In contrast, where shallow peat exists, warming and underlying permafrost thaw can cause the
108 active layer to deepen into mineral horizons with low C:N ratios. This can lead to flow paths of
109 groundwater being directed through these mineral horizons leading to an increased adsorption of
110 DON and release of nitrate through subsequent mineralization and nitrification (Harms *et al.*, 2013).
111 This process can occur to a lesser extent on a seasonal cycle with groundwater influx from mineral
112 horizons in the winter and surface runoff from organic horizons in spring and summer. Extensive
113 future permafrost thaw in catchments is expected to increase the seasonal groundwater contribution
114 leading to decreased DON concentrations and increased nitrate concentrations in streams and rivers
115 (Walvoord and Striegl, 2007).

116 These studies focus on gradual active layer deepening processes. Other more rapid permafrost
117 degradation processes such as riverine and coastal erosion are more spatially limited but could be
118 responsible for moving nitrogen species rapidly and directly from terrestrial permafrost to riverine
119 or coastal environments (Berhe *et al.*, 2007). This mechanism is understudied so the resulting
120 nitrogen export is still relatively unknown.

121 The processing and cycling of nitrogen that occurs in-stream and in near-shore coastal areas after
122 release from permafrost is also largely unknown. DON represents a 5x greater influx to Arctic shelf
123 waters from rivers than nitrate across the whole Arctic but 70% of the DON is removed in shelf
124 waters before reaching the open marine environment (Thibodeau *et al.*, 2017). The processes
125 involved in this removal are largely unclear but riverine nitrate can have a strong remineralised
126 signal, with sources from recycling of particulate organic nitrogen (PON) and DON (Thibodeau
127 *et al.*, 2017). The biolability of riverine DON and exchanges with the nitrate pool are key aspects that



128 influence the Arctic nitrogen cycle, and the impact of future permafrost thaw on these aspects has
129 not been studied. This study focusses solely on the dissolved species of nitrogen, where most
130 cycling occurs.

131 These dissolved flux changes and alterations to cycling processes due to permafrost thaw could
132 have substantial impacts on the productivity of Arctic marine ecosystems and on element cycling
133 within the Arctic Ocean (Dittmar and Kattner, 2003) with potential global scale implications. It is
134 important, therefore, to understand how permafrost degradation may influence each nitrogen
135 species input across multiple Arctic river catchments and the subsequent potential changes to the
136 riverine and coastal nitrogen cycle as a result.

137 In this study, dual stable nitrogen and oxygen isotopes of dissolved nitrate ($\delta^{15}\text{N-NO}_3^-$ and $\delta^{18}\text{O-NO}_3^-$),
138 and nitrogen isotopes of TDN and DON ($\delta^{15}\text{N-TDN}$ and $\delta^{15}\text{N-DON}$) were used to determine
139 cycling and source processes. During various cycling stages of the nitrogen cycle, biological
140 processes favour the use of the light nitrogen isotope (^{14}N) over the heavy isotope (^{15}N) due to it
141 being more energetically favourable (Sigman and Casciotti, 2001). This leaves the residual pool
142 with more of the heavier isotopes thus a more positive (higher) isotopic signature. The relative
143 extent of a certain cycling processes is proportional to the residual isotopic signature.
144 Transformation between nitrogen pools can also induce kinetic isotopic fractionation with
145 fractionation factors unique to each transformation process (Voigt *et al.*, 2017). Oxygen isotopes
146 behave similarly but have different sources to nitrogen during each cycling stage so the use of the
147 dual isotope technique can distinguish sources of nitrate and determine the relative influence of
148 nitrogen cycling processes such as nitrification, assimilation or denitrification (Thibodeau *et al.*,
149 2017). Comparisons of $\delta^{15}\text{N-NO}_3^-$ versus $\delta^{18}\text{O-NO}_3^-$ can show distinct sources of nitrate and mixing
150 between them based on the environmental conditions inducing specific isotopic fractionations to
151 both elements. Additionally, particular nitrogen cycling processes can be shown using this method.
152 For example, during the nitrate consumption processes of denitrification or biological assimilation,
153 the residual pools of nitrogen and oxygen become enriched in the heavy isotopes equally (Granger
154 *et al.*, 2004), the fractionation of the two isotopes is “coupled” resulting in a near 1:1 relationship
155 (Botrel *et al.*, 2017). In comparison, nitrification, a nitrate producing process, causes decoupled
156 fractionation between the isotopes due to different nitrogen and oxygen sources (Sigman *et al.*,
157 2005).

158 Since DON concentrations are elevated relative to nitrate concentrations in this Arctic riverine
159 environment (Thibodeau *et al.*, 2017), $\delta^{15}\text{N-DON}$ can be determined, allowing the possible sources
160 of DON to be determined and when combined with nitrate isotopes data, some of the cycling
161 mechanisms can also be identified. This is only the second study utilising $\delta^{15}\text{N-DON}$ in the Arctic
162 (Thibodeau *et al.*, 2017) and the first to apply it to Arctic rivers.

163 This study aims to contribute to the debate on the role of permafrost degradation on changing
164 riverine loads of nitrogen into the Arctic. Specifically determining if there is an increase of
165 dissolved nitrogen supply into Arctic rivers and coastal zones as a result of permafrost thawing
166 within catchments, what the proportions of nitrogen species within these inputs are and whether a
167 unique permafrost thaw signal be detected in rivers using dissolved nitrogen species. A major focus
168 was on the understudied area of nitrogen cycling within rivers and coastal areas. Nitrogen isotope
169 signals in thaw zones and Arctic rivers with differing permafrost extents were utilised to provide



170 insights into catchment scale nitrogen cycling and recycling of various forms during riverine
171 transport.

172 **2 Methods**

173 **2.1 Study areas and sample collection**

174 *2.1.1 Kolyma*

175 Samples from the lower Kolyma River catchment were used to identify local scale nitrogen signals
176 from zones affected by varying levels of permafrost thaw (Figure 1a). Samples were collected in
177 September 2018 from surface water, filtered on-site using a 0.7µm glass fibre filter and immediately
178 frozen. Late Autumn sampling was chosen as active layer depths reach their maximum extent at
179 this time, allowing the greatest permafrost DOM influx to streams (Schoor *et al.*, 2008; Mann *et*
180 *al.*, 2012).

181 PT1 is a well-studied permafrost thaw zone known as Duvannyi Yar, where a 10-12km long outcrop
182 of permafrost is exposed along the bank of the Kolyma River. The permafrost is part of the
183 extensive Pleistocene Yedoma permafrost that covers much of the Kolyma and Lena catchments
184 and contains almost a third of all organic matter stored in Arctic permafrost (Vonk *et al.*, 2013).
185 Limited freeze-thaw action prevents processing and degradation of organic matter, resulting in
186 storage of ancient and well-preserved organic matter. Ancient ice wedges also characterise this
187 permafrost, accounting for about 50% of the soil volume and storing some of the organic matter
188 within it (Schirmer *et al.*, 2011). Yedoma permafrost is mostly intact throughout the Kolyma
189 catchment except at a limited number of erosional sites such as Duvannyi Yar. Here, the river erodes
190 it at 100m per year, leading to extensive permafrost degradation throughout the soil horizon
191 (Vasil'chuk *et al.*, 2001). This destabilizes soil profiles, leading to bank collapses and release of
192 thaw-water and ancient organic matter into streams. Radiocarbon dating of DOC collected from a
193 fluid mud stream draining from the thawing permafrost yielded an age of 20,000 years at this site.
194 This organic matter is highly biolabile after thawing occurs and can be assimilated rapidly by
195 aquatic microorganisms after mineralisation (Vonk *et al.*, 2012; Spencer *et al.*, 2015). Samples at
196 this site were collected from a fluid mud stream draining the thawing permafrost.

197 In contrast, samples PI1 and PI2 were taken from streams draining sites underlain with intact
198 modern permafrost with little permafrost derived DOC, if any. The sites contained functioning
199 ecosystems of larch forests, shrub/moss and lichen understory with no exposed permafrost (Lorant
200 *et al.*, 2018). This is representative of large areas of the Kolyma catchment as well as portions of
201 other Russian Arctic Rivers so can be used to determine the background non-thaw signal for
202 nitrogen species.

203 To determine how nitrogen species from permafrost thaw are processed within an Arctic river and
204 a marine environment, samples were taken in the main stem of the Kolyma River, downstream of
205 the thaw site along with samples in the estuarine zone where the Kolyma River meets the East
206 Siberian Sea (Figure 1a).

207 *2.1.2 Pan-Arctic Rivers*

208 The Arctic Great Rivers Observatory (ArcticGRO) (<https://arcticgreatrivers.org/>) is an international
209 project collecting and analysing riverine water samples using identical methods. Samples used in
210 this study were collect in 2017 using methods described in Holmes *et al.*, (2018) from the six largest
211 Arctic rivers, four in Russia: Kolyma, Ob', Lena and Yenisey and two in North America: Yukon



212 and Mackenzie (Figure 1b). Together, the proportion of continuous and discontinuous permafrost
213 within these catchments is 48%, similar to the proportions across the whole pan-Arctic catchments
214 (52%) (Tank *et al.*, 2012). Thus, these rivers represent overall pan-Arctic conditions. These
215 catchments also cover transitions from continuous permafrost zones of the Arctic to permafrost
216 free, capturing variability that occurs across the pan-Arctic (Tank *et al.*, 2012). Studying the major
217 Arctic rivers allowed comparisons of nitrogen loading and cycling between rivers to identify
218 variations of permafrost and catchment influences. The generated datasets from this study were
219 interpreted using discharge, concentration and other biogeochemical data from 2003 to 2018,
220 available on the ArcticGRO website (<https://arcticgreativers.org/data/>).



221

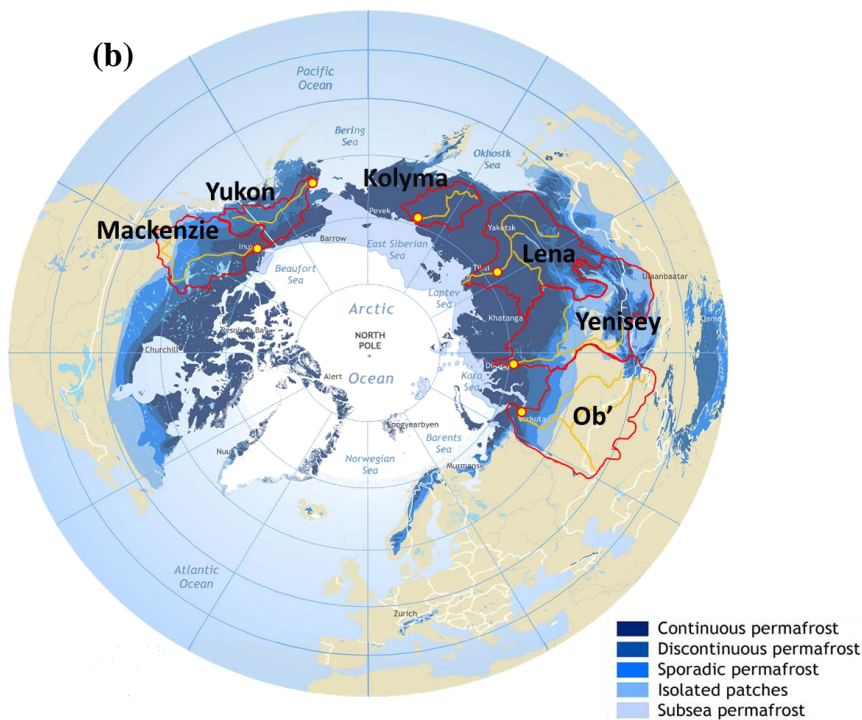
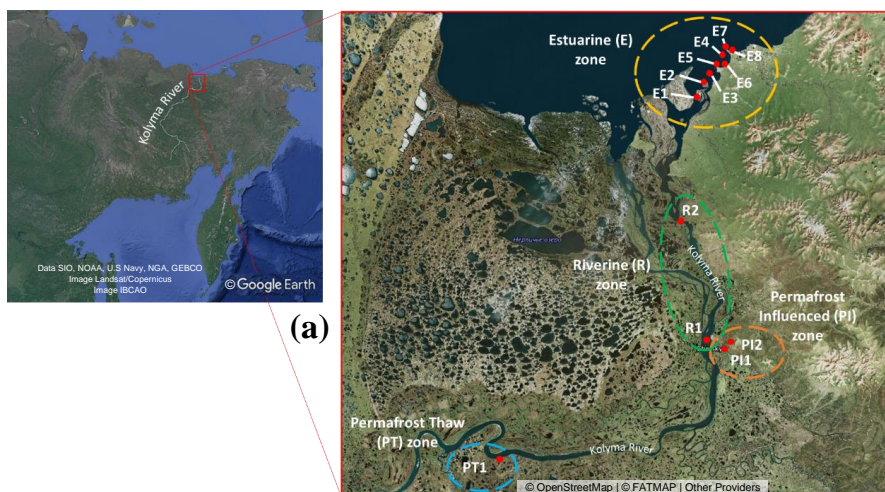


Figure 1 – (a) Sample names and collection locations from sites around the lower Kolyma River and estuary. Samples collected on a research trip in autumn 2018. Satellite image 1 source: Data SIO, NOAA, U.S Navy, NGA, GEBCO / Image Landsat/Copernicus | Image IBCAO. © Google Earth. Satellite image 2 source: © OpenStreetMap | © FATMAP | Other Providers.

(b) Catchment areas (red lines) and sampling locations (red and yellow circles) of the six largest Arctic rivers (orange lines) used in the ArcticGRO III project. The extent and type of permafrost present in each catchment is also shown. Base map modified from Brown et al. (1997).



222 **2.2 Analysis of nitrogen species - concentrations and stable isotopes**

223 TDN and DOC concentrations were measured using a Shimadzu TOC/TN analyser at the
224 University of Edinburgh (Kolyma samples) and Woods Hole Research Centre (ArcticGRO
225 samples). Inorganic nutrient concentrations were measured at the Woods Hole Research Centre
226 using an Astoria Analyzer (ArcticGRO samples) and also calculated from mass spectrometer peak
227 areas referenced to two internal standards with known concentrations and isotopic values (Kolyma
228 samples). All stable isotopic analysis was carried out at the School of Geosciences, University of
229 Edinburgh.

230 **2.3 $\delta^{15}\text{N}$ and $\delta^{18}\text{O}$ of Nitrate (NO_3^-)**

231 The dual isotope technique to measure nitrogen and oxygen isotopes of nitrate was carried out by
232 the denitrifier method modified from Sigman *et al.*, (2001); Casciotti *et al.*, (2002) and McIlvin and
233 Casciotti, (2011). It utilises denitrifying bacteria, *Pseudomonas aureofaciens*, which lack nitrous
234 oxide (N_2O) reductase activity to convert dissolve nitrate into N_2O gas while maintaining an
235 identical nitrogen isotopic signature to the original nitrate. The oxygen isotope signature is subject
236 to change with water molecules so is corrected for using the method in Weigand *et al.*, (2016).
237 Samples with low nitrate concentrations ($<1\mu\text{M}$) could not be analysed for nitrate isotopes. As a
238 result, some samples were excluded from analysis. The analytical precision for $\delta^{15}\text{N}\text{-NO}_3^-$ was
239 $\pm 0.4\text{‰}$ and $\pm 0.3\text{‰}$ for the two reference standards IAEA-N3 and USGS-34 respectively and for
240 $\delta^{18}\text{O}\text{-NO}_3^-$ it was $\pm 1.0\text{‰}$ and $\pm 0.8\text{‰}$ respectively. This was based on >30 measurements of the
241 international standards analysed on several different days.

242 **2.4 $\delta^{15}\text{N}$ of TDN**

243 This method utilises an extra step prior to the denitrifier method where the sample TDN is converted
244 into nitrate while maintaining the TDN isotopic signature. This involves oxidation with potassium
245 persulphate followed by digestion of the organic nitrogen to an equivalent amount of nitrate that is
246 then prepared via the denitrifier method. This procedure was adapted from Knapp *et al.*, (2005) and
247 Thibodeau *et al.*, (2013, 2017). $\delta^{15}\text{N}\text{-TDN}$ isotopic values represent the values of both DON and
248 DIN (nitrate + nitrite). Therefore, $\delta^{15}\text{N}\text{-DON}$ is calculated using concentration weighted $\delta^{15}\text{N}\text{-NO}_3^-$
249 and $\delta^{15}\text{N}\text{-TDN}$ values and allowed the processes involved in organic and inorganic nitrogen to be
250 compared. $\delta^{15}\text{N}\text{-DON}$ could only be calculated when $\delta^{15}\text{N}\text{-NO}_3^-$ values were available ($[\text{NO}_3^-] >$
251 $1\mu\text{M}$). Samples with nitrate concentrations less than $1\mu\text{M}$ were reported as $\delta^{15}\text{N}$ of TDN since $\delta^{15}\text{N}$
252 of DON was not calculable and using $\delta^{15}\text{N}$ of TDN allowed comparisons with other samples.

253

254 This calculation assumes that the isotopic signature of nitrate can represent that of DIN and the
255 contribution from ammonium is negligible. This is because ammonium is unstable in peatland
256 environments and is rapidly converted into nitrate, meaning nitrate makes up the majority of the
257 DIN pool and ammonium concentrations are low and often below detection limits. (Holmes *et al.*,
258 2012b).



259 **3 Results and Discussion**
260 **3.1 Permafrost extent and nitrogen species**

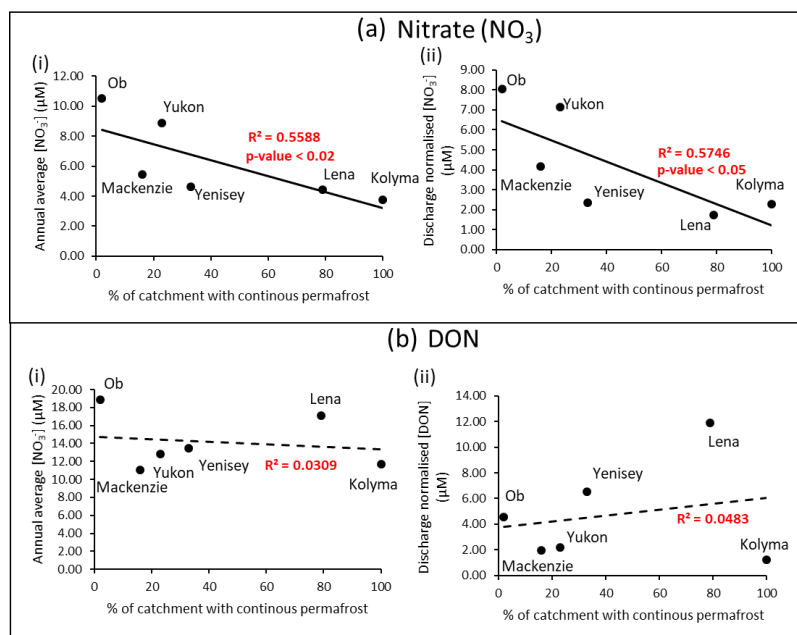


Figure 2 - Relationships between the extent of continuous permafrost within each river catchment and (a) nitrate and (b) DON (i) concentrations (μM) and (ii) discharge normalised concentrations (μM). Data from the ArcticGRO online dataset.

261 Mean ArcticGRO nitrate and DON (TDN-DIN) concentrations of all available data points in the
262 ArcticGRO dataset from 2003 - 2018 were calculated for each of the six rivers. This produced
263 average annual nitrate and DON concentrations, which was plotted against the percentage of
264 continuous permafrost in each river catchment (Figure 2 (a) (i) and (b) (i)) (from Holmes et al.,
265 2012). To remove the effect of unequal seasonal sampling and the large variability in hydrology in
266 these river systems, the concentrations were normalised to the discharge of the sample collection
267 month and plotted against percentage continuous permafrost (Figure 2 (a) (b) - (ii)). This allowed
268 more accurate inter-river comparisons of nitrogen species concentration.

269 Negative correlations are present between permafrost extent and nitrate concentrations.
270 Concentration trends shown are statistically significant between 95 to 98% confidence levels (p -
271 value = 0.05 to 0.02) according to the Spearman's rank test. However, no statistically significant
272 relationship exists between DON concentrations and permafrost extent for all rivers. The strongest
273 correlation is for the nitrate concentration versus permafrost extent, with a strong negative
274 relationship at a 98% confidence level ($p\text{-value} < 0.02$).

275 Overall, these negative linear relationships suggest that the less permafrost present in a river
276 catchment, the more nitrate is released from the surrounding soil. Therefore, permafrost degradation
277 may induce greater concentrations of nitrate into Arctic rivers. Similar trends have been observed
278 in other studies (Jones *et al.*, 2005; Harms *et al.*, 2013). Conversely, no significant relationship can
279 be observed between DON concentrations and permafrost extent in any of the plots ((b) - (i) or
280 (ii)). Given that DON is the dominant form of nitrogen released from soil, the increase in nitrate



281 concentrations but not DON suggests that cycling of organic nitrogen to inorganic forms in soils
 282 and/or upstream rivers may be promoted with decreasing permafrost extents. Figure 2 displays the
 283 variability from the extent of continuous permafrost, but not from active permafrost degradation.
 284 Local scale measurements of thaw sites from the Kolyma River will be used in the following section
 285 to address if active permafrost thaw releases nitrogen and identify cycling processes involved.
 286 Seasonal trends will be used to see when each of the species become dominant and use this to help
 287 determine catchment-scale processes.

288 3.2 Local scale permafrost degradation signals

289 3.2.1 Concentration of nitrogen species

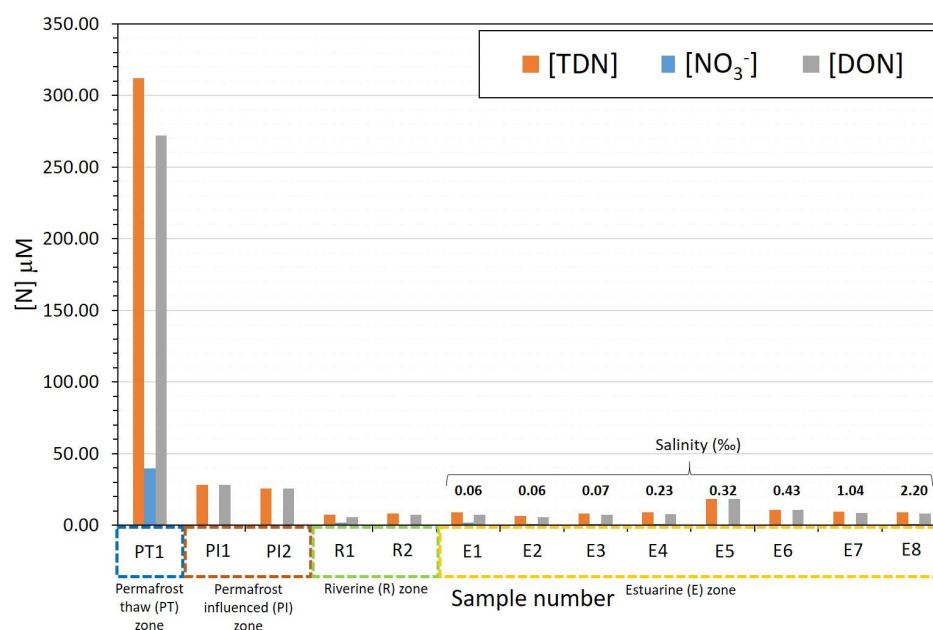


Figure 3 - Concentrations of Total Dissolved Nitrogen [TDN], Nitrate [NO₃⁻] and Dissolved Organic Nitrogen [DON] in different zones of the lower Kolyma River as overviewed in Figure 1 (a). Salinity values are displayed for the estuarine samples in order of increasing salinity.

290 Figure 3 shows the concentrations of different nitrogen species in zones of the Kolyma River and
 291 estuary. The concentrations of nitrate and DON represent the dissolved inorganic and the dissolved
 292 organic species of TDN respectively. Site PT1 at Duvannyi Yar, with substantial permafrost thaw,
 293 has greatly elevated concentrations of all nitrogen species in comparison to other samples. Most of
 294 the nitrogen is present as DON (312μM for DON and 40μM for nitrate). In comparison, the
 295 permafrost influenced zone (where intact permafrost is present), has substantially lower
 296 concentrations with DON roughly 25-28μM and nitrate concentrations being almost negligible at
 297 0.2μM. The amount of DON relative to nitrate in these sites was however much greater than the
 298 permafrost thaw site. Permafrost degradation appears to release DON and nitrate in large amounts
 299 whereas the intact permafrost releases much less DON and very little nitrate.

300 In the main stem of the river, DON concentrations decreased (to 6-7μM). Nitrate concentrations
 301 were greater than in the permafrost-influenced zone (1-2μM) but still an order of magnitude lower
 302 than the thaw zone. In the estuarine zone, concentrations of both DON and nitrate fluctuated slightly



303 but remained at a similar level to the riverine samples (DON = 5-9 μ M, nitrate = 0.2-2 μ M) with no
304 clear trend in concentration with increasing salinity. DON increased slightly in site 007 but this was
305 anomalous in comparison with the rest of the site concentrations.

306 These trends suggest that within intact permafrost zones of the Kolyma catchment, only DON is
307 released from soil in significant amounts. DON concentrations were 169x greater than nitrate
308 concentrations. This observation that more permafrost leads to less release of nitrate supports
309 observations on the catchment-scale as noted in section 3.1. Our findings show that within the
310 Yedoma permafrost thaw zone, permafrost degradation facilitates the release of large amounts of
311 both nitrate and DON from the soil and into the dissolved phase. DON was still the dominant
312 species, but not as much as with intact permafrost, with a concentration 7 times greater than nitrate.

313 However, in the main stem of the river, the signals were quickly lost, with concentrations decreasing
314 by 44 and 31-fold for nitrate and DON respectively. This decrease in both species was partially due
315 to a dilution effect but could also be due to the diluting source having a lower proportion of nitrate
316 than DON. Such a possibility is consistent with intact continuous permafrost occupying the vast
317 majority of the catchment with smaller inputs of DON and with lower DON: nitrate ratios. DON
318 concentrations may be 10-times higher than nitrate concentrations in the main stem due to nitrate
319 being more readily removed than DON. However, there was no clear change in concentrations
320 downriver, suggesting processing of the nitrogen pool may be small but cycling processes are
321 difficult to determine using only concentration data.



322 3.2.2 Nitrogen Isotopic signatures

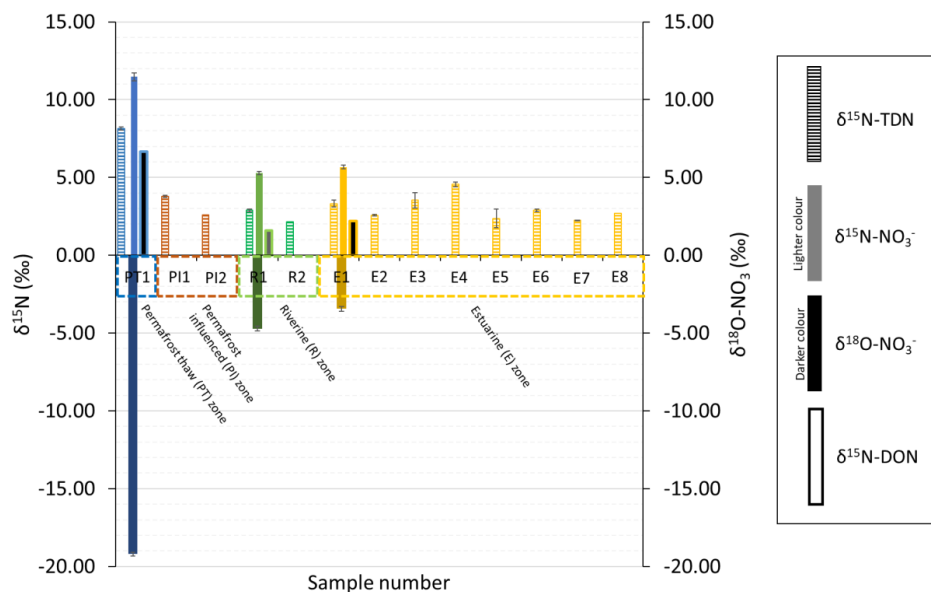


Figure 4 - Nitrogen isotopes of TDN, Nitrate (NO_3^-) and DON in different zones of the lower Kolyma River as overviewed in Figure 1(a). Oxygen isotopes ($\delta^{18}\text{O}$) of nitrate are also shown on the negative scale below the nitrogen isotope values. Only three sites (PT1, R1 & R2) were able to have nitrogen isotopes of nitrate (and therefore also of DON) analysed as most nitrate concentrations were $<1\mu\text{M}$. However, since nitrate concentrations were very small in comparison to DON (see Figure 3) – especially for the permafrost influenced site, then it can be assumed that the nitrogen isotopic signature of DON is roughly equal to the signature of TDN ($\delta^{15}\text{N-DON} \approx \delta^{15}\text{N-TDN}$). The permafrost-influenced sample was analysed across four repeat runs allowing a robust standard deviation to be calculated.

323 Figure 4 shows the stable isotopic signatures of different nitrogen species in zones along the
324 Kolyma River. At the permafrost thaw site, nitrogen isotopes of all species were enriched in ^{15}N
325 ($\delta^{15}\text{N-NO}_3^- = 12\text{‰}$, $\delta^{15}\text{N-DON} = 7\text{‰}$) and $\delta^{18}\text{O-NO}_3^-$ values were very negative at -19‰ . In
326 comparison, the permafrost influenced sites had lower isotopic values for DON (3 to 4‰).

327 The signals observed in the permafrost thaw site were rapidly lost in the main stem of the river and
328 into the estuary. In the river, $\delta^{15}\text{N-NO}_3^-$ was $\sim 5\text{‰}$ and $\delta^{15}\text{N-DON}$ was 2 to 5‰, while $\delta^{18}\text{O-NO}_3^-$
329 was around -5‰ . At the start of the estuary, $\delta^{18}\text{O-NO}_3^-$ increased to -3‰ . With consideration of the
330 errors associated with the measurement, there were no clear trends observed for $\delta^{15}\text{N}$ moving
331 downstream (similar to the concentration data) and into the estuary, suggesting minimal alterations
332 to dominant processing cycles of nitrogen in the main river stem.

333 In summary, a unique signal representing inputs from thawing Yedoma permafrost was detected
334 using concentrations and isotopic signatures of nitrogen species (Figure 3 and Figure 4). From the
335 site at Duvannyi Yar, extensive permafrost thaw brings water to the Kolyma River with very high
336 DON concentrations ($272\mu\text{M}$) and high $\delta^{15}\text{N-DON}$ (6.7‰). In addition, nitrate concentrations were
337 high ($40\mu\text{M}$) with very high $\delta^{15}\text{N-NO}_3^-$ ($11.5 \pm 0.26\text{‰}$) but very low $\delta^{18}\text{O-NO}_3^-$ ($-19.2 \pm 0.37\text{‰}$).

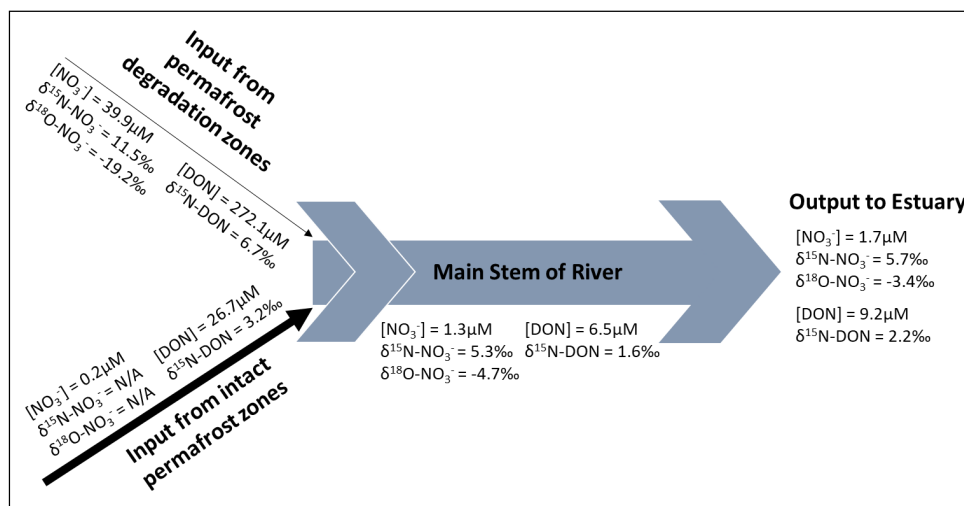


Figure 5 – Summary of concentration and isotopic signals of nitrate and DON species in the Kolyma system. Data displayed are average values of all samples in each zone of the river

3.2.3 Explanation of signals observed and likely processing

During degradation, permafrost releases large amounts of organic matter and organic nitrogen (DON) from the soil and ice (272 μM in this study, Figure 5). This undergoes rapid mineralization, firstly to highly reactive ammonium then to nitrate via nitrification (Voigt *et al.*, 2017). The lighter isotope of nitrogen is preferred for these reactions through kinetic fractionation (Mariotti *et al.*, 1981), however the first step of this reaction (ammonification, DON converted to ammonium), is associated with a small fractionation factor (Swart *et al.*, 2008) so cannot fully explain the high isotopic signature of the residual DON pool (6.7‰). Nitrification produces high concentrations of nitrate (40 μM), however the waterlogged and anaerobic conditions in the soil, combined with the lack of vascular plants for competition (Repo *et al.*, 2009), produces good conditions for denitrifying bacteria to convert the readily available nitrate to atmospheric N₂ via denitrification. This reaction produces much stronger kinetic fractionation than nitrification (Swart *et al.*, 2008) so this partial denitrification, where not all nitrate is denitrified, results in the residual nitrate pool becoming isotopically heavy with a high δ¹⁵N-NO₃⁻ signal of 11.5‰. DON also shows this high denitrification signal suggesting exchange of denitrified nitrogen between the nitrate and DON pools through the assimilation of partially denitrified heavy nitrate and the production of heavy DON by remineralisation. Even though ¹⁴N is preferred to form DON, a highly invigorated nitrogen cycle with continuous nitrogen exchange between pools explains the unusually heavy δ¹⁵N values in both DON and nitrate pools.

Additionally, the fact that DON is not isotopically heavier than nitrate is also expected as the primary source of DON is from decaying organic matter preserved in the permafrost and this process releases lower δ¹⁵N that forms DON (Sipler and Bronk, 2015). This is supplemented with a smaller contribution from DON formed from the recycled heavy nitrate. Therefore, nitrogen processing in the permafrost thaw zone not only involves active release of DON by heterotrophic remineralisation with anaerobic processes such as denitrification, but also exchange between nitrogen pools. Oxygen isotopes of nitrate provide further evidence for this recycling.

364



365 During denitrification, fractionation of nitrogen and oxygen is 1:1; therefore, oxygen isotopes
366 should behave similarly to nitrogen isotopes and become isotopically heavy (high signal) in the
367 residual nitrate pool (Sigman *et al.*, 2009). This is not observed however, as $\delta^{18}\text{O}\text{-NO}_3^-$ in the thaw
368 stream had a very negative (low) signal (-19.2‰). Therefore, denitrification alone cannot explain
369 the oxygen isotopic signatures. The $\delta^{18}\text{O}\text{-NO}_3^-$ signal ‘resets’ to the value of ambient water when it
370 is recycled (Buchwald and Casciotti, 2010) while the fixed nitrogen is internally cycled, retaining
371 its isotopic signatures (Sigman *et al.*, 2009). The observed $\delta^{18}\text{O}\text{-NO}_3^-$ signal in the permafrost thaw
372 zone is very close to the value of $\delta^{18}\text{O}\text{-H}_2\text{O}$ of Kolyma River water for this time of year (-20‰) (Yi
373 *et al.*, 2012). However, this stream water was draining straight from the ancient ice wedges and had
374 not been in contact with the main stem ‘modern’ water. The $\delta^{18}\text{O}\text{-H}_2\text{O}$ of ice wedges was much
375 lower than present day river $\delta^{18}\text{O}\text{-H}_2\text{O}$: -33.3‰ (Vonk *et al.*, 2013) due to different environmental
376 conditions during the formation period of this permafrost (Hubberten *et al.*, 2004; Vonk *et al.*,
377 2013). Given that the denitrification signal was largely reduced in $\delta^{18}\text{O}\text{-NO}_3^-$ suggests that the
378 partially denitrified nitrate was almost completely recycled through the assimilation-
379 ammonification-nitrification cycle during permafrost thaw. This vigorous nitrogen cycling and
380 exchange between nitrogen pools should occur in the thaw site soil before reaching the river.
381 Collectively, the dual nitrogen and oxygen isotopic signals of nitrate and nitrogen isotopes of DON
382 provide evidence for a range of nitrogen recycling process active in the thaw zone. This produced
383 unusually heavy $\delta^{15}\text{N}$ values in both DON and nitrate pools and a $\delta^{18}\text{O}\text{-NO}_3^-$ signal representing
384 both the recycling and denitrification processes. These isotopic signals show a unique signature
385 where inputs from Yedoma permafrost degradation enter the main stem of the river. Processing in
386 the main stem can then alter these signals, explaining the signal observed at the river mouth.

387 Organic matter from this permafrost site is very biolabile and ancient permafrost DOC is the most
388 biolabile source of DOC in riverine Arctic systems due to lack of processing and survival of bacteria
389 (Vonk *et al.*, 2013). Up to 50% of permafrost DOC can be lost in less than seven days in the Kolyma
390 River (Spencer *et al.*, 2015). This time period is equal to water residence times between headwater
391 streams in thaw zones and the river mouth (3 days) (Vonk *et al.*, 2013). However, DON may behave
392 differently to DOC in terms of cycling. Unlike DOC (where a large proportion of the carbon is
393 oxidised and lost as CO_2) (O’Donnell *et al.*, 2016), DON will mostly be converted into nitrate
394 during degradation. This nitrate will likely continue to be recycled along with DON degradation in
395 the river.

396 Therefore, it is expected that the high $\delta^{15}\text{N}$ values (for both DON and nitrate) from the thaw site
397 would be retained through recycling and even if some nitrogen was lost as N_2 or N_2O or to PON
398 (which sinks out) via assimilation the residual dissolved pool would remain isotopically heavy.
399 However, since these DON signals were not clearly observed downstream this suggests that the
400 contributions of these thaw streams were relatively small compared to other DON sources in the
401 main stem of the river (Drake *et al.*, 2018) probably receiving waters from intact continuous
402 permafrost, resulting in nitrogen signals from permafrost thaw being quickly lost. Dilution with
403 main stem water containing lower concentrations and lower $\delta^{15}\text{N}$ values is a major contributor to
404 the changes observed.

405 The main stem isotopic signatures represent the average catchment characteristics (a combination
406 of all permafrost influenced and thaw sites) and since the $\delta^{15}\text{N}\text{-TDN}$ were much more similar (the
407 same within error) to the permafrost influenced site, it can be assumed that these conditions
408 represent the majority of the Kolyma catchment as it has near 100% continuous permafrost



409 coverage. However, within that TDN input, permafrost influenced sites supply mostly DON but
410 very little nitrate (Figure 2 and Figure 3). From the permafrost zone to the main stem, DON
411 concentrations decreased and nitrate concentrations increased slightly (even with dilution effects).
412 The isotopic signature of the main stem nitrate was also significantly heavier than that of permafrost
413 and main stem DON. The concentration trends suggest that recycling of DON to nitrate was
414 occurring in the river and, when combined with the isotopic trends, some of the isotopically heavy
415 nitrogen from DON and nitrate originating in the thaw site may have contributed to these recycling
416 processes. This allows the heavy nitrogen signal from the thawing Yedoma permafrost to be
417 transferred and retained in the main stem nitrate. This was assisted by the negligible diluting nitrate
418 inputs from much of the permafrost-covered catchment. Importantly, this also suggests that a
419 significant nitrate pool in the main stem is produced from DON recycling rather than from direct
420 nitrate inputs to the river.

421 However, $\delta^{18}\text{O}-\text{NO}_3^-$ values in the main stem were higher than the thaw site (-3.4 to -4.7‰). These
422 values were much greater than would be expected from nitrogen recycling and nitrate/DON
423 exchange occurring in the main stem. Determining the cause for these high signals is difficult due
424 to a multitude of possible factors influencing the isotopic signatures. Co-occurrence of partial
425 nitrate uptake and nitrification in the main stem which decouples the nitrogen and oxygen isotopes
426 (Sigman *et al.*, 2009) may be occurring but would only account for a $\delta^{18}\text{O}-\text{NO}_3^-$ increase of around
427 5‰ (Wankel *et al.*, 2007). External sources such as atmospheric deposition and surface runoff with
428 minimal interaction with catchment soils (e.g. snowmelt or high riverine discharge during sampling
429 due to localised rainfall) may also bring high $\delta^{18}\text{O}-\text{NO}_3^-$ and lower $\delta^{15}\text{N}-\text{DON}$ values into the main
430 stem (Heikoop *et al.* (2015), Thibodeau *et al.* (2017)). However, the amount of atmospheric $\delta^{18}\text{O}-$
431 NO_3^- signal that reaches the main stem may be low as studies have shown that nearly all snowpack
432 nitrate is assimilated or remineralised before being released into the river, thus losing nearly all the
433 high $\delta^{18}\text{O}-\text{NO}_3^-$ signal (Tye and Heaton, 2007).

434 Overall, determining the cause of the high $\delta^{18}\text{O}-\text{NO}_3^-$ values and lower $\delta^{15}\text{N}-\text{DON}$ in the main stem
435 relative to the permafrost zone cannot be constrained with this study, but is likely to be some
436 combination of atmospheric, microbial and recycling signals with co-occurrence of uptake,
437 nitrification and possible denitrification. All of these may change seasonally which is explained in
438 greater depth in section 3.3.

439 In summary, a unique signature representing inputs from thawing Yedoma permafrost was
440 identified in the lower Kolyma River catchment indicating anaerobic degradation, denitrification,
441 and vigorous nitrogen cycling within permafrost soils undergoing thaw. Dilution of the DON thaw
442 signal occurs in the main stem but the DON (from the thaw site as well as the surrounding
443 catchment) also undergoes mineralisation to nitrate, transferring the isotopic thaw signature to the
444 nitrate. Therefore, increases in the nitrogen release from Yedoma permafrost soils, irrespective of
445 the species, is most likely to be reflected in riverine nitrate concentrations. However, signals are
446 unlikely to be strongly observed around the mouth of rivers unless very spatially extensive thaw
447 zones are present in the catchment providing large enough fluxes of nitrogen species liberated from
448 permafrost. This would allow the degradation signal to persist through the background catchment-
449 wide nitrogen signal from modern surface soils.

450 The permafrost thaw occurring at this Kolyma site is only one type of degradation mechanism that
451 can occur. It involves erosion of ice rich permafrost (Yedoma) found mainly in the Lena and



452 Kolyma catchments but not in other Russian Arctic river catchments such as the Ob' and Yenisey
 453 (Wild *et al.*, 2019) (some is also present in the Yukon catchment). This type of degradation produces
 454 a greater export in the form of POC than DOC (Wild *et al.*, 2019), as seen in the Kolyma and Lena.
 455 This preferred release of POC (thus PON) from Yedoma permafrost could partially explain why a
 456 stronger degradation signal was not observed downstream in the Kolyma River. Other thaw
 457 mechanisms such as top-down active layer deepening occur widely across the Ob' and Yenisey
 458 catchments and produce significantly more thaw sourced DOC than POC (Wild *et al.*, 2019), and
 459 possibly more DON than PON.

460
 461 Large seasonality of DOC permafrost contribution exists in Arctic rivers (Wild *et al.*, 2019).
 462 Permafrost derived DOC had a greater contribution to total DOC flux in all four rivers in late
 463 autumn and winter compared to spring and summer when modern DOC sources dominate export.
 464 A similar mechanism may also operate for DON where the sources in spring and summer are not
 465 derived as strongly from permafrost but from surface soils that experience minimal nitrogen
 466 processing. Therefore, permafrost signals and associated processes should be considered on spatial
 467 (inter-catchment) and temporal scales.
 468

469 3.3 Seasonal nitrogen species trends in rivers

470 3.3.1 Time series concentration and discharge trends

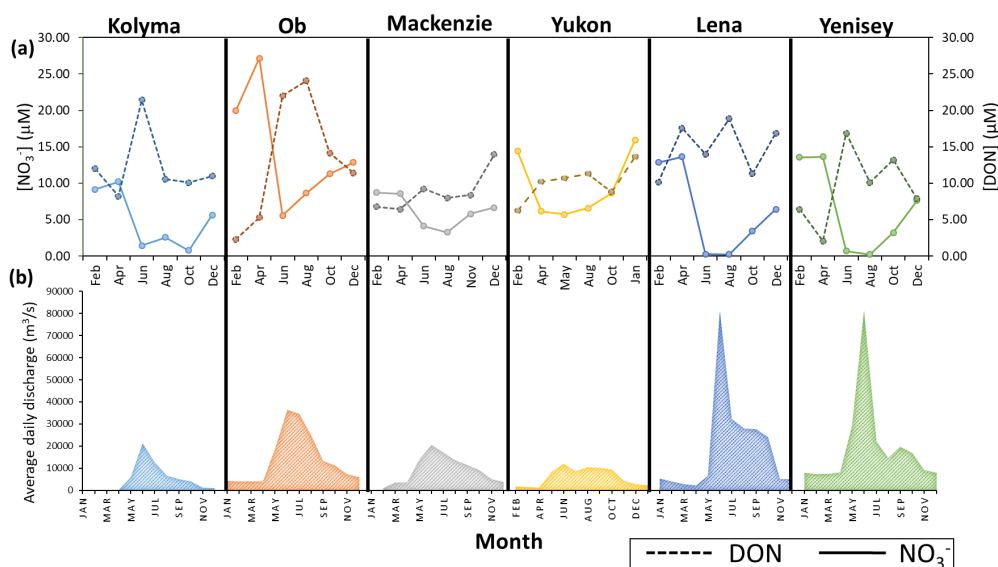


Figure 6 - Seasonal concentrations (a) for nitrate and DON in the six Arctic GRO rivers. Discharge trends for each river are also shown in (b). Note, sample concentration values were taken six times throughout the year, every second month. The daily discharges for each month were averaged to produce the average daily discharge value for each month, 12 per year. Data obtained from the ArcticGRO online database.

471 Figure 6(b) shows that all six rivers follow a similar seasonal discharge trend typical of northern
 472 high-latitude rivers. Low flow is present in winter months, where groundwater is the primary source
 473 of water. During spring, snowmelt causes rapid increases in discharge (the spring freshet) peaking
 474 in late May to June. Peaks are greatest in the Lena and Yenisey. After the freshet, discharge



475 decreases throughout summer, occurring more rapidly in the Lena and Yenisey, while in other
 476 rivers, peak discharge extends throughout summer, most apparent in the Yukon River.

477 All rivers in general show increases in DON concentrations [DON] in summer months during peak
 478 discharge and this concentration increase is highest in the Ob' followed by the Yenisey and Kolyma
 479 and lowest in the Lena, Mackenzie and Yukon where only small seasonal changes occur in [DON].
 480 Nitrate concentrations [NO₃⁻] in most rivers show opposite seasonal trends to [DON] (Figure 6 (a))
 481 with the Ob' showing the greatest seasonal change of all rivers in both nitrate and DON. The Lena
 482 and Yenisey show nitrate concentrations decreasing to almost zero in the summer months during
 483 peak discharge.

484 In general, Figure 6 confirms that DON is the dominant form of nitrogen released from these soils
 485 and transported in these rivers, due to its high concentration during the high discharge periods of
 486 the spring freshet. This DON source is likely derived from surface runoff through organic rich top
 487 soil (Harms *et al.*, 2013). Following the local scale Kolyma section, seasonal stable isotopes trends
 488 are used next to detect (1) permafrost degradation signals and (2) any in-stream processing of
 489 nitrogen.

490

491 3.3.2 Time series nitrogen isotopic trends

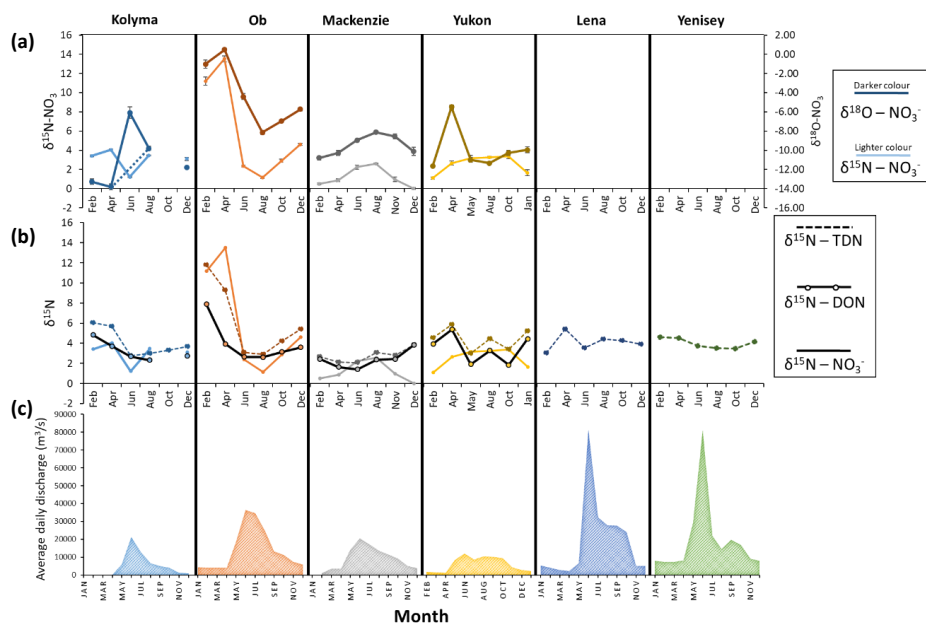


Figure 7 - Seasonal nitrogen (and oxygen) isotopic trends for all six Arctic GRO rivers. Nitrate isotopes as part of the dual isotope technique ($\delta^{15}\text{N}$ and $\delta^{18}\text{O}$) are shown on (a). Nitrogen isotopes of TDN, nitrate and DON, note the one scale for all three, are shown on (b). Seasonal discharges are also shown on (c). Only $\delta^{15}\text{N}$ values of TDN were plotted for the Lena and Yenisey since nitrate concentrations were very low for dual isotopic analysis of nitrate, hence $\delta^{15}\text{N}-\text{NO}_3^-$ and $\delta^{18}\text{O}-\text{NO}_3^-$ values were not obtained. However, since nitrate concentrations were very small in comparison to DON (see Figure 6) then it can be assumed that the nitrogen isotopic signature of DON is approximately equal to the signature of TDN ($\delta^{15}\text{N}-\text{DON} \approx \delta^{15}\text{N}-\text{TDN}$)

492 Figure 7 presents a time series isotopic analysis of the Arctic rivers. The sampling sites were located
 493 at the mouths of the rivers, therefore they integrate signals of various source of nitrogen and
 494 nitrogen cycling processes in the catchment (Figure 1). From Figure 6 and Figure 7, strong seasonal



495 variations affect nearly all the trends of nitrogen species in each river, but the trends suggest that
496 discharge was not the greatest influencer on the isotopic signatures. Summer values of $\delta^{15}\text{N}$ of
497 nitrate, DON and TDN are around 2 to 4‰, similar to the Kolyma River main stem in summer,
498 indicating a mixed nitrogen source dominated by surface nitrogen sources diluting signals from
499 intact permafrost and permafrost degradation signals (Figure 7). These results are consistent with
500 previous studies of DOC in Arctic rivers (Wild *et al.*, 2019). Permafrost derived DOC has a greater
501 contribution to total DOC flux in all four rivers in late autumn and winter compared to spring and
502 summer when modern DOC sources dominate export. A similar mechanism may also operate for
503 DON where the sources in spring and summer are not derived as strongly from permafrost but from
504 surface soils that experience minimum nitrogen processing.

505 $\delta^{15}\text{N-NO}_3^-$ and $\delta^{15}\text{N-DON}$ values of the Kolyma and Ob' in late winter and early spring are high
506 before becoming lower in spring/summer and returning to high values at the end of the year (Figure
507 7) (this is also seen in the Yukon to a lesser extent). It is notable that the Kolyma and Ob' have the
508 highest and lowest continuous permafrost extent respectively among the large Arctic rivers. We
509 evaluate the seasonal trend further in the Ob' River (with comparison to the Kolyma), which has
510 the largest seasonal isotopic shift out of all the rivers (Figure 7).

511 3.3.3 *Relating seasonal trends to nitrate sources, permafrost thaw and nitrogen cycling* 512 *mechanisms*

513 The Ob' has the greatest seasonal isotopic shifts with very heavy winter $\delta^{15}\text{N-NO}_3^-$ values of 12 to
514 14‰ occurring over winter and early spring but decreasing to 2‰ in summer and a change from 8
515 to 2.5‰ for $\delta^{15}\text{N-DON}$. The $\delta^{18}\text{O-NO}_3^-$ trend for the Ob' River follows a similar pattern to the $\delta^{15}\text{N-NO}_3^-$
516 (i.e. they are coupled). However, for the Kolyma, the two isotopes are decoupled and show
517 strong opposing trends, though this trend could be influenced by the anomalously high $\delta^{18}\text{O-NO}_3^-$
518 value in June and may not represent true conditions.

519 The peak $\delta^{15}\text{N-NO}_3^-$ values in the Ob' river are similar to the signal for denitrification in high-
520 latitude permafrost regions (Harms *et al.*, 2013) and the isotopic and nitrate concentration peak in
521 winter could be further evidence of extensive denitrification sources. Despite low concentrations of
522 DON during the winter months, its isotopic signature was similar to the Kolyma thaw site, however
523 the higher values of $\delta^{15}\text{N-NO}_3^-$ suggests that different processes are occurring in each river and that
524 the signal cannot be compared to the possible permafrost thaw signal observed in the Kolyma
525 (section 3.2.3). The stronger denitrification signal may be more visible in the main stem of the Ob'
526 unlike in the Kolyma due to a much lower extent of continuous permafrost within the catchment
527 (permafrost present as discontinuous or sporadic under the large peatland of Western Siberian
528 Lowlands (Wild *et al.*, 2019)). The lack of permafrost in the Ob' catchment may also allow some
529 groundwater encroachment of the mineral horizon in some places within the catchment. Here DON
530 can be adsorbed and mineralised to nitrate (Harms *et al.*, 2013). Denitrification of this
531 remineralised nitrate due to the waterlogging of the soil in these large wetlands would also lead to
532 the high isotopic signatures observed. It is important to note that these denitrification processes
533 occur without permafrost thaw influence in the Ob' whereas the denitrification signal observed in
534 the Kolyma Yedomas thaw site was likely due to the permafrost degradation. Denitrification signals
535 are much more influential in the Ob' than the Kolyma where the permafrost extent is very low. The
536 high nitrate concentrations show that a substantial amount of denitrified nitrate is added to the rivers
537 and the Ob' River is displaying a source-dominated signal, with instream processes possibly less
538 influential.



539 The coupling of $\delta^{15}\text{N-NO}_3^-$ and $\delta^{15}\text{N-DON}$ throughout the year suggests the same source for both
540 nitrogen species. However, some DON may also be oxidised into nitrate in the main stem and allow
541 the heavy $\delta^{15}\text{N}$ signal to be transferred from the DON to the nitrate. This would also reduce the
542 DON concentrations as observed.

543

544 The observed variability of nitrate isotopes in the Ob' River can be approximated to changes
545 between two dominant sources as outlined in Figure 8. The heavier winter $\delta^{15}\text{N-NO}_3^-$ values in the
546 Ob' represent groundwater dominated sources and the high $\delta^{18}\text{O-NO}_3^-$ values are largely coupled
547 to the $\delta^{15}\text{N-NO}_3^-$ (Figure 7). This is further evidence for denitrification in the consistently wet
548 conditions of the Ob' catchment, preventing significant recycling of the denitrified nitrate and
549 resetting of the $\delta^{18}\text{O-NO}_3^-$ to $\delta^{18}\text{O-H}_2\text{O}$. (Frey and McClelland, 2009). Additionally, the lack of
550 permafrost allows more percolation of groundwater in winter and a greater input of a denitrified
551 signal. The lower $\delta^{15}\text{N-NO}_3^-$ summer values were consistent with minimally processed atmospheric
552 nitrogen sources, with little denitrified nitrate present, delivered through surface runoff during the
553 spring freshet to the river. However, the lower $\delta^{18}\text{O-NO}_3^-$ values in the summer do not correspond
554 to an influence of an isotopically high atmospheric or snowmelt nitrate source. This could be due
555 to the main stem summer signal being a mix of different sources and recycling occurring (as
556 described previously for the local scale Kolyma catchment). The $\delta^{18}\text{O-NO}_3^-$ values are lower and
557 closer to the $\delta^{18}\text{O-H}_2\text{O}$ values of the Ob' (14.85‰) (Yi *et al.*, 2012), than seen in the Kolyma,
558 suggesting some degree of nitrate recycling that can cause $\delta^{18}\text{O-NO}_3^-$ values to be reset to water
559 values. These values are likely mixed with surface runoff signals from snowmelt (bringing higher
560 $\delta^{18}\text{O-NO}_3^-$ signals) and near surface runoff through topsoil, masking the smaller input of
561 denitrification signals from groundwater.

562 A regression line between the two different sources in the Ob' (Figure 8) shows the dominant source
563 changing throughout the year and main-stem water showing mixing between them. Overall, it is
564 likely that the groundwater derived signal is present throughout the year as part of a mixed signal
565 but the seasonal variation of dominant sources influences its visibility in the main stem. Surface
566 spring/summer flows dominate and mask the groundwater signal during summer whereas in winter
567 the subsurface flow is dominant and allows the groundwater and associated denitrified signal to be
568 more clearly observed

569 The Kolyma seasonal trend is similar to the Ob' except the magnitude of isotopic and concentration
570 change was less (Figure 7). $\delta^{18}\text{O-NO}_3^-$ was decoupled from the $\delta^{15}\text{N-NO}_3^-$ in the Kolyma, unlike
571 the coupling in the Ob. The continuous permafrost coverage preventing catchment-wide
572 denitrification in the Kolyma along with the observed conversion of DON to nitrate and subsequent
573 recycling could explain the decoupling throughout the year. This decoupling also suggests that
574 nitrate uptake is low and the small contribution of nitrate due to the high continuous permafrost
575 extent is likely to drive nitrate limitation in this river, despite DON remineralisation (Figure 2,
576 section 3.2.3). This similar but suppressed trend suggests that the denitrification signal is less
577 influential and was diluted, similar to local-scale observations (section 3.2). The greater coverage
578 of permafrost in the Kolyma catchment compared to the Ob' may reduce the seasonal change in
579 nitrogen species signals, especially nitrate (as observed in Figure 2) by restricting flow-paths to
580 minimal contact with mineral horizons and reducing groundwater flow. This can also explain the
581 observed mixing line and the surface source dominance throughout the year shown in Figure 8.



582

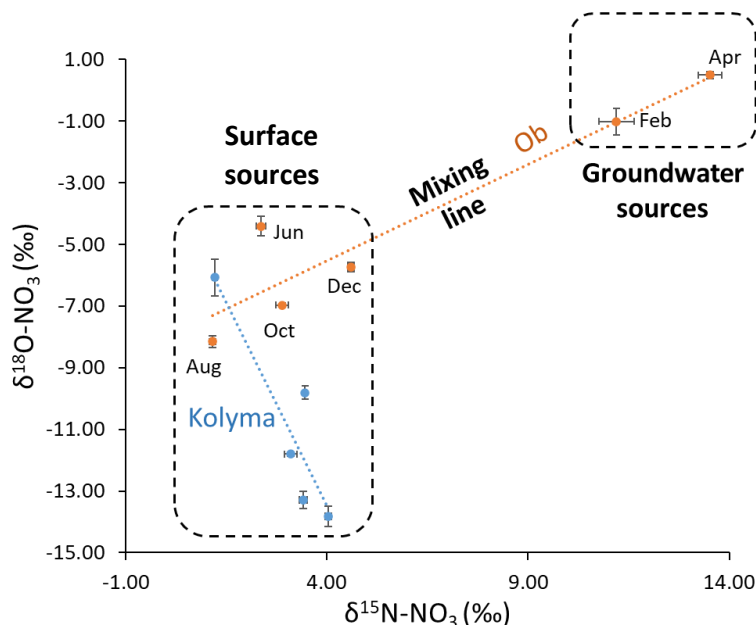


Figure 8 – Different sources of nitrate throughout the year in the Ob' and Kolyma catchments inferred by relationships between $\delta^{15}\text{N-NO}_3^-$ and $\delta^{18}\text{O-NO}_3^-$. A mixing line can be plotted as a regression line between the two sources. The location on the plot that each sample occurs can indicate the dominant nitrate sources at that time and from that, the processes occurring can be inferred.

583 The local scale permafrost degradation signals observed from the Yedoma permafrost degradation
584 in the Kolyma may be visible in the seasonal trends due to similar main stem DON and nitrate
585 signals in the early season, possibly assisted by the lack of other nitrate inputs and DON recycling
586 to nitrate. However, it is not possible to observe any permafrost degradation signals in the Ob'
587 catchment or to compare trends with previous local scale findings due to the dominance of the
588 groundwater derived denitrification signal and different catchment conditions.

589 3.3.4 Explanations for times series trends in other Arctic rivers

590 The Mackenzie and Yukon show $\delta^{15}\text{N-NO}_3^-$ trends peaking in the summer months (Figure 7). This
591 was an opposite trend to the nitrate concentration, and more closely follows the discharge trends.
592 The Yukon had the most prolonged $\delta^{15}\text{N-NO}_3^-$ peak out of all the rivers. Little change in $\delta^{15}\text{N-DON}$
593 occurred for the Mackenzie while for the Yukon it showed variability all year with no clear trends,
594 $\delta^{18}\text{O-NO}_3^-$ was strongly coupled to $\delta^{15}\text{N-NO}_3^-$ for the Mackenzie but was uncoupled for the Yukon.

595 In the Mackenzie River, the source signal in the summer months is dominated by runoff, carrying
596 a large DON signal. However, since DON isotopes and concentrations are decoupled from nitrate
597 isotopes and concentrations, the factors influencing both nitrogen species are different. Nitrate is
598 influenced mainly by instream processes (Harms *et al.*, 2013) due to assimilation or uptake of nitrate
599 by phytoplankton in summer. The smaller isotopic shift between seasons could also signify
600 assimilation rather than denitrification (Struck, 2012). This process would be assisted by the large
601 area of lakes in the Mackenzie catchment where water residence times are increased allowing
602 extensive primary productivity (Janjua and Tallman, 2015).



603 The Yukon followed similar trends to the Mackenzie (for $\delta^{15}\text{N}$, $[\text{NO}_3^-]$, $[\text{DON}]$) suggesting uptake
604 in the summer months was also a dominant nitrogen cycling process. Similarly, there is extensive
605 lake cover in the Yukon catchment (Brabets *et al.*, 2000). However, $\delta^{18}\text{O}-\text{NO}_3^-$ and $\delta^{15}\text{N}-\text{NO}_3^-$ were
606 uncoupled and variable, potentially reflecting different sources of water throughout the year and
607 the extended discharge period providing water involved in nitrate processing with different $\delta^{18}\text{O}-$
608 H_2O values.

609 It was difficult to determine any dominant processes within the Lena and Yenisey due to the lack
610 of nitrate isotopic data and the little seasonal change in $\delta^{15}\text{N}-\text{TDN}$ (DON). However, a unique
611 aspect of these rivers is the very high freshet discharge and the associated high DON concentrations
612 but very low nitrate concentrations. The fact that these large changes in runoff can occur without a
613 change in isotopic DON could suggest that recent topsoil derived organic matter was the dominant
614 source of nitrogen throughout the year, similar to observations for carbon (Wild *et al.*, 2019).

615 **3.4 Implications of findings and possible future changes**

616 Permafrost thaw will have different impacts of riverine nitrogen geochemistry in different
617 catchments across the Arctic. With future permafrost degradation, through both active layer
618 deepening and erosional degradation, the seasonal trends may change from the Kolyma style more
619 towards the Ob' style since the Ob' represents a catchment with very little permafrost present.
620 Greater shifts in concentrations and $\delta^{15}\text{N}$ isotopic signals between seasons would be expected with
621 high $\delta^{15}\text{N}$ signals in the winter and early spring through denitrification of waterlogged soil but a
622 rapid shift in $\delta^{15}\text{N}$ with runoff conditions. However, this would depend on other catchment
623 conditions as well as the style of thaw and the rate of degradation.

624 As thaw released DON was observed to be converted to nitrate in the main stem of the Kolyma and
625 likely in other rivers, this would increase the amount of bioavailable nitrogen (nitrate is more
626 bioavailable for assimilation than DON) and possibly fuel increased productivity. As observed in
627 the study, this conversion would have the greatest impact in catchments with few other nitrate
628 inputs, e.g. from high continuous permafrost coverage, such as the Kolyma. However, if active
629 layer deepening induces the widespread reduction of continuous permafrost extent in favour of
630 discontinuous coverage, this may allow nitrogen input processes similar to those described for the
631 Ob' to dominate over this main stem mineralisation of nitrate for the long term.

632 This study demonstrates that nitrate concentrations may increase the most relative to other nitrogen
633 species and would carry with it a high isotopic signature from denitrification processes. This
634 increase of nitrate is supported by other studies such as Walvoord and Striegl (2007) but not by
635 Frey *et al.* (2007) who predict an increase in DON not nitrate. There is ongoing debate over the
636 dominant species likely to be observed.

637 Irrespective of N species released and the thaw mechanism, nitrogen fluxes are likely to increase
638 with permafrost degradation causing significant impact to the coastal zones. Any increases in
639 nitrogen loading to coastal Arctic areas will have large impacts on productivity since these zones
640 are heavily nitrogen limited (Thibodeau *et al.*, 2017). Currently, productivity peaks over a short
641 period in summer when light is not limiting. However, permafrost thaw and greater nitrogen fluxes
642 may increase the magnitude of these productivity peaks inducing possible algal blooms. Yet, light
643 limitation will still control productivity later in the year. Overall, the cycling of these nitrogen
644 species in coastal zones is essential to understand further to make robust predictions of future
645 change.



646 **4 Conclusions**

647 Overall, catchment permafrost coverage seems to control main stem nitrate concentrations but not
648 DON, with large extents of continuous permafrost leading to low concentrations of nitrate in Arctic
649 rivers. In local Kolyma degradation sites, Yedoma permafrost thaw was characterised by high DON
650 and nitrate concentrations, high $\delta^{15}\text{N}$ -DON and $\delta^{15}\text{N}$ - NO_3^- and very low $\delta^{18}\text{O}$ - NO_3^- . These
651 signatures indicate rapid recycling and exchange between nitrogen pools resulting in the entire
652 system becoming isotopically heavy for nitrogen. Upon release to the main river stem, this signature
653 is greatly diluted but evidence for recycling of thaw derived DON to nitrate, transferring the heavy
654 isotopic signature to nitrate, was observed. This DON recycling could be the main source of nitrate
655 in catchments with extensive permafrost coverage and few nitrate inputs. However, these input
656 signals from Yedoma thaw are unlikely to be observed strongly at the river mouth unless thaw
657 zones are more spatially extensive.

658 $\delta^{15}\text{N}$ of nitrate, TDN and DON during summer and spring freshets generally exhibit values around
659 2 to 4‰, DON dominates the nitrogen export within these rivers, in the form of fresh DON derived
660 from surface runoff through modern, organic rich topsoil. However, Arctic rivers all have different
661 nitrogen dynamics based on their catchment characteristics. The Ob' catchment, with its lowest
662 extent of permafrost coverage and extensive peatland area demonstrates a strong denitrification
663 signal, however this cannot be linked to the thaw induced denitrification signal observed in the
664 Kolyma. The Ob' isotopic signal is strongly seasonal and influenced by the changing soil flow paths
665 that arise throughout the year. The Kolyma had a similar seasonal trend but with reduced magnitude
666 and showed evidence of differing processes occurring compared to the Ob' but were similar to local
667 scale observations. A diluted denitrification signal, DON recycling to nitrate and low nitrate uptake
668 were all possibly assisted by the lack of other nitrate inputs and high permafrost coverage. In other
669 Arctic river catchments, different factors can mask any fresh permafrost thaw signals. Lacustrine
670 nitrogen assimilation and uptake are dominant in the Mackenzie and seasonal changes in water
671 sources are important for the Yukon catchment while large freshet discharges in the Lena and
672 Yenisey likely inundate the catchments with runoff-derived nitrogen.

673 It is possible that with future decreases in catchment permafrost coverage, seasonal nitrogen
674 dynamics in Arctic rivers could begin to resemble that of the Ob' catchment. In general, increased
675 fluxes of nitrogen are expected as a result of thaw which would have impacts on coastal
676 environments and ecosystems, as well as in rivers with nitrogen limitation. However, the extent of
677 this is unclear at present. Further studies are required to explore more local scale and coastal
678 nitrogen cycling and the impacts of permafrost thaw on riverine and coastal environments.

679 This study shows how nitrogen isotopes can be used to integrate catchment wide processes in Arctic
680 rivers as well as showcasing small scale nitrogen dynamics within permafrost degradation zones.
681 Utilising this technique across further sites in the Arctic will help to further our understanding of
682 current processes and future changes in Arctic nitrogen cycling.

683 **5 Data Availability**

684 Data will be made available on a public repository upon final publication.

685 **6 Author Contributions**

686 AF carried out laboratory work and wrote the manuscript. RSG designed of the study and helped
687 with the interpretation of the data. RET assisted with laboratory work. Both RSG and RET



688 contributed to the writing of the manuscript. JR and RGMS collected samples from the Kolyma and
689 provided further information on the sites in the lower Kolyma catchment. RMH manages the online
690 Arctic GRO dataset used for this project made available the ArcticGRO samples. CM led and
691 coordinated the CAO, ARISE project. All authors provided comments on the manuscript.

692 **7 Conflict of Interest Statement**

693 The authors declare that the research was conducted in the absence of any commercial or financial
694 relationships that could be construed as a potential conflict of interest.

695 **8 Acknowledgements**

696 We thank the ArcticGRO consortia for providing Pan-Arctic river samples and datasets. We also
697 extend thanks to the ARISE consortia and the NERC's Changing Arctic Ocean (CAO) programme,
698 particularly Louisa Norman and Antonia Doncila for logistic support. Thanks are also due to Colin
699 Chilcott for isotopic analysis at the University of Edinburgh.

700 **9 Funding**

701 This work resulted from the ARISE project (NE/P006310/1 awarded to RSG), part of the Changing
702 Arctic Ocean programme, jointly funded by the UKRI Natural Environment Research Council
703 (NERC) and the German Federal Ministry of Education and Research (BMBF).

704 **10 References**

- 705 Anderson, L. G. *et al.* (2011) 'East Siberian Sea, an Arctic region of very high biogeochemical
706 activity', *Biogeosciences*, 8(6), pp. 1745–1754. doi: 10.5194/bg-8-1745-2011.
- 707 Anisimov, O. and Reneva, S. (2006) 'Permafrost and changing climate: the Russian perspective.',
708 *Ambio*, 35(4), pp. 169–75. Available at: <http://www.ncbi.nlm.nih.gov/pubmed/16944641>
709 (Accessed: 28 November 2018).
- 710 Berhe, A. A. *et al.* (2007) 'The Significance of the Erosion-induced Terrestrial Carbon Sink',
711 *BioScience*. Narnia, 57(4), pp. 337–346. doi: 10.1641/B570408.
- 712 Botrel, M. *et al.* (2017) 'Assimilation and nitrification in pelagic waters: insights using dual nitrate
713 stable isotopes ($\delta^{15}\text{N}$, $\delta^{18}\text{O}$) in a shallow lake', *Biogeochemistry*. Springer International
714 Publishing, 135(3), pp. 221–237. doi: 10.1007/s10533-017-0369-y.
- 715 Brabets, T., Wang, B. and Meade, R. (2000) *Environmental and Hydrologic Overview of the Yukon*
716 *River Basin, Alaska and Canada Water-Resources Investigations Report 99-4204*. Anchorage.
717 Available at: <https://pubs.usgs.gov/wri/wri994204/pdf/wri994204.pdf> (Accessed: 4 June 2019).
- 718 Brown, J. *et al.* (1997) *Circum-Arctic map of permafrost and ground-ice conditions, Circum-*
719 *Pacific Map*. doi: 10.3133/cp45.
- 720 Buchwald, C. and Casciotti, K. L. (2010) 'Oxygen isotopic fractionation and exchange during
721 bacterial nitrite oxidation', *Limnology and Oceanography*. John Wiley & Sons, Ltd, 55(3), pp.
722 1064–1074. doi: 10.4319/lno.2010.55.3.1064.
- 723 Casciotti, K. L. *et al.* (2002) 'Measurement of the Oxygen Isotopic Composition of Nitrate in
724 Seawater and Freshwater Using the Denitrifier Method'. American Chemical Society. doi:
725 10.1021/AC020113W.
- 726 Chadburn, S. E. *et al.* (2017) 'An observation-based constraint on permafrost loss as a function of
727 global warming', *Nature Climate Change*. Nature Publishing Group, 7(5), pp. 340–344. doi:
728 10.1038/nclimate3262.
- 729 Dittmar, T. and Kattner, G. (2003) 'The biogeochemistry of the river and shelf ecosystem of the



- 730 Arctic Ocean: A review', *Marine Chemistry*, 83(3–4), pp. 103–120. doi: 10.1016/S0304-
731 4203(03)00105-1.
- 732 Drake, T. W. *et al.* (2018) 'The Ephemeral Signature of Permafrost Carbon in an Arctic Fluvial
733 Network', *Journal of Geophysical Research: Biogeosciences*, 123(5), pp. 1475–1485. doi:
734 10.1029/2017JG004311.
- 735 Farquharson, L. M. *et al.* (2019) 'Climate Change Drives Widespread and Rapid Thermokarst
736 Development in Very Cold Permafrost in the Canadian High Arctic', *Geophysical Research Letters*.
737 John Wiley & Sons, Ltd, 46(12), pp. 6681–6689. doi: 10.1029/2019GL082187.
- 738 Frey, K. E. *et al.* (2007) 'Impacts of climate warming and permafrost thaw on the riverine transport
739 of nitrogen and phosphorus to the Kara Sea', *Journal of Geophysical Research: Biogeosciences*.
740 Wiley-Blackwell, 112(G4), p. n/a-n/a. doi: 10.1029/2006JG000369.
- 741 Frey, K. E. and McClelland, J. W. (2009) 'Impacts of permafrost degradation on arctic river
742 biogeochemistry', *Hydrological Processes*. Wiley-Blackwell, 23(1), pp. 169–182. doi:
743 10.1002/hyp.7196.
- 744 Frey, K. E. and Smith, L. C. (2005) 'Amplified carbon release from vast West Siberian peatlands
745 by 2100', *Geophysical Research Letters*. John Wiley & Sons, Ltd, 32(9), p. L09401. doi:
746 10.1029/2004GL022025.
- 747 Granger, J. *et al.* (2004) 'Coupled nitrogen and oxygen isotope fractionation of nitrate during
748 assimilation by cultures of marine phytoplankton', *Limnology and Oceanography*. John Wiley &
749 Sons, Ltd, 49(5), pp. 1763–1773. doi: 10.4319/lo.2004.49.5.1763.
- 750 Harms, T. K. *et al.* (2013) *Permafrost thaw and a changing nitrogen cycle*. Available at:
751 https://www.lter.uaf.edu/sympo/2013/FRI-1045_Harms.pdf (Accessed: 27 August 2019).
- 752 Hassol, S. *et al.* (2004) *Impacts of a warming Arctic: Arctic Climate Impact Assessment*.
753 Cambridge University Press. Available at: [https://www.amap.no/documents/doc/impacts-of-a-
754 warming-arctic-2004/786](https://www.amap.no/documents/doc/impacts-of-a-warming-arctic-2004/786) (Accessed: 22 November 2018).
- 755 Heikoop, J. M. *et al.* (2015) 'Isotopic identification of soil and permafrost nitrate sources in an
756 Arctic tundra ecosystem', *Journal of Geophysical Research: Biogeosciences*, 120(6), pp. 1000–
757 1017. doi: 10.1002/2014JG002883.
- 758 Holmes, R. M. *et al.* (2000) 'Flux of nutrients from Russian rivers to the Arctic Ocean: Can we
759 establish a baseline against which to judge future changes?', *Water Resources Research*, 36(8), pp.
760 2309–2320. doi: 10.1029/2000WR900099.
- 761 Holmes, R. M. *et al.* (2012a) 'Seasonal and Annual Fluxes of Nutrients and Organic Matter from
762 Large Rivers to the Arctic Ocean and Surrounding Seas', *Estuaries and Coasts*, 35(2), pp. 369–
763 382. doi: 10.1007/s12237-011-9386-6.
- 764 Holmes, R. M. *et al.* (2012b) 'Seasonal and Annual Fluxes of Nutrients and Organic Matter from
765 Large Rivers to the Arctic Ocean and Surrounding Seas', *Estuaries and Coasts*. Springer-Verlag,
766 35(2), pp. 369–382. doi: 10.1007/s12237-011-9386-6.
- 767 Holmes, R. M. *et al.* (2018) *ArcticGRO - Metadata*. Available at:
768 https://drive.google.com/file/d/1mCCIdeN6z4RyYuKRGsvinKwIK_rIR1pu/view.
- 769 Hubberten, H. W. *et al.* (2004) 'The periglacial climate and environment in northern Eurasia during
770 the Last Glaciation', *Quaternary Science Reviews*. Pergamon, 23(11–13), pp. 1333–1357. doi:
771 10.1016/J.QUASCIREV.2003.12.012.
- 772 Janjua, M. Y. and Tallman, R. F. (2015) *A mass-balanced Ecopath model of Great Slave Lake to*



- 773 support an ecosystem approach to fisheries management: Preliminary results, Canadian Technical
774 Report of Fisheries and Aquatic Sciences. Winnipeg. Available at:
775 <https://pdfs.semanticscholar.org/f34d/8748a5885b2a1b4a50edfbc01f97f4c5dbfe.pdf> (Accessed:
776 27 August 2019).
- 777 Jones, J. B. *et al.* (2005) 'Nitrogen loss from watersheds of interior Alaska underlain with
778 discontinuous permafrost', *Geophysical Research Letters*. John Wiley & Sons, Ltd, 32(2), p.
779 L02401. doi: 10.1029/2004GL021734.
- 780 Knapp, A. N., Sigman, D. M. and Lipschultz, F. (2005) 'N isotopic composition of dissolved
781 organic nitrogen and nitrate at the Bermuda Atlantic Time-series Study site', *Global
782 Biogeochemical Cycles*. Wiley-Blackwell, 19(1). doi: 10.1029/2004GB002320.
- 783 Lobbes, J. M., Fitznar, H. P. and Kattner, G. (2000) 'Biogeochemical characteristics of dissolved
784 and particulate organic matter in Russian rivers entering the Arctic Ocean', *Geochimica et
785 Cosmochimica Acta*, 64(17), pp. 2973–2983. doi: 10.1016/S0016-7037(00)00409-9.
- 786 Loranty, M. M. *et al.* (2018) 'Understory vegetation mediates permafrost active layer dynamics and
787 carbon dioxide fluxes in open-canopy larch forests of northeastern Siberia', *PLoS ONE*, 13(3), pp.
788 1–17. doi: 10.1371/journal.pone.0194014.
- 789 MacLean, R. *et al.* (1999) 'The effect of permafrost on stream biogeochemistry: A case study of
790 two streams in the Alaskan (U.S.A.) taiga', *Biogeochemistry*. Kluwer Academic Publishers, 47(3),
791 pp. 239–267. doi: 10.1007/BF00992909.
- 792 Mann, P. J. *et al.* (2012) 'Controls on the composition and lability of dissolved organic matter in
793 Siberia's Kolyma River basin', *Journal of Geophysical Research: Biogeosciences*, 117(1), pp. 1–
794 15. doi: 10.1029/2011JG001798.
- 795 Mann, P. J. *et al.* (2015) 'Utilization of ancient permafrost carbon in headwaters of Arctic fluvial
796 networks', *Nature Communications*. Nature Publishing Group, 6, pp. 1–7. doi:
797 10.1038/ncomms8856.
- 798 Mariotti, A. *et al.* (1981) 'Experimental determination of nitrogen kinetic isotope fractionation:
799 Some principles; illustration for the denitrification and nitrification processes', *Plant and Soil*.
800 Kluwer Academic Publishers, 62(3), pp. 413–430. doi: 10.1007/BF02374138.
- 801 McClelland, J. W. *et al.* (2006) 'A pan-arctic evaluation of changes in river discharge during the
802 latter half of the 20th century', *Geophysical Research Letters*, 33(6), p. L06715. doi:
803 10.1029/2006GL025753.
- 804 McCrackin, M. L., Harrison, J. A. and Compton, J. E. (2014) 'Factors influencing export of
805 dissolved inorganic nitrogen by major rivers: A new, seasonal, spatially explicit, global model',
806 *Global Biogeochemical Cycles*. Wiley-Blackwell, 28(3), pp. 269–285. doi:
807 10.1002/2013GB004723.
- 808 McIlvin, M. R. and Casciotti, K. L. (2011) 'Technical Updates to the Bacterial Method for Nitrate
809 Isotopic Analyses', *Analytical Chemistry*, 83(5), pp. 1850–1856. doi: 10.1021/ac1028984.
- 810 Nelson, F. E. *et al.* (1997) 'Estimating Active-Layer Thickness over a Large Region: Kuparuk River
811 Basin, Alaska, U.S.A.', *Arctic and Alpine Research*, 29(4), p. 367. doi: 10.2307/1551985.
- 812 NOAA (2014) *Next Steps in Arctic Governance | Council of Councils*. Available at:
813 <https://councilofcouncils.cfr.org/global-memos/next-steps-arctic-governance> (Accessed: 5
814 September 2019).
- 815 NSIDC (2018) *Climate and Frozen Ground | National Snow and Ice Data Center*. Available at:
816 <https://nsidc.org/cryosphere/frozenground/climate.html> (Accessed: 5 September 2019).



- 817 O'Donnell, J. A. *et al.* (2016) 'Dissolved organic matter composition of Arctic rivers: Linking
818 permafrost and parent material to riverine carbon', *Global Biogeochemical Cycles*, 30(12), pp.
819 1811–1826. doi: 10.1002/2016GB005482.
- 820 Peterson, B. J. *et al.* (2002) 'Increasing River Discharge to the Arctic Ocean', *Science*, 298(5601),
821 pp. 2171–2173. doi: 10.1126/science.1077445.
- 822 Repo, M. E. *et al.* (2009) 'Large N₂O emissions from cryoturbated peat soil in tundra', *Nature*
823 *Geoscience*. Nature Publishing Group, 2(3), pp. 189–192. doi: 10.1038/ngeo434.
- 824 Schirrmeister, L. *et al.* (2011) 'Sedimentary characteristics and origin of the Late Pleistocene Ice
825 Complex on north-east Siberian Arctic coastal lowlands and islands – A review', *Quaternary*
826 *International*. Pergamon, 241(1–2), pp. 3–25. doi: 10.1016/J.QUAINT.2010.04.004.
- 827 Schuur, E. A. G. *et al.* (2008) 'Vulnerability of Permafrost Carbon to Climate Change: Implications
828 for the Global Carbon Cycle', *BioScience*. Narnia, 58(8), pp. 701–714. doi: 10.1641/B580807.
- 829 Schuur, E. A. G. *et al.* (2009) 'The effect of permafrost thaw on old carbon release and net carbon
830 exchange from tundra', *Nature*. Nature Publishing Group, 459(7246), pp. 556–559. doi:
831 10.1038/nature08031.
- 832 Sigman, D. M. *et al.* (2001) 'A Bacterial Method for the Nitrogen Isotopic Analysis of Nitrate in
833 Seawater and Freshwater'. American Chemical Society. doi: 10.1021/AC010088E.
- 834 Sigman, D. M. *et al.* (2005) 'Coupled nitrogen and oxygen isotope measurements of nitrate along
835 the eastern North Pacific margin', *Global Biogeochemical Cycles*. John Wiley & Sons, Ltd, 19(4),
836 p. n/a-n/a. doi: 10.1029/2005GB002458.
- 837 Sigman, D. M. *et al.* (2009) 'The dual isotopes of deep nitrate as a constraint on the cycle and
838 budget of oceanic fixed nitrogen', *Deep Sea Research Part I: Oceanographic Research Papers*.
839 Pergamon, 56(9), pp. 1419–1439. doi: 10.1016/J.DSR.2009.04.007.
- 840 Sigman, D. M. and Casciotti, K. L. (2001) 'NITROGEN ISOTOPES IN THE OCEAN'. doi:
841 10.1006/rwos.2001.0172.
- 842 Sipler, R. E. and Bronk, D. A. (2015) 'Dynamics of Dissolved Organic Nitrogen', *Biogeochemistry*
843 *of Marine Dissolved Organic Matter*. Academic Press, pp. 127–232. doi: 10.1016/B978-0-12-
844 405940-5.00004-2.
- 845 Spencer, R. G. M. *et al.* (2015) 'Detecting the signature of permafrost thaw in Arctic rivers', pp. 1–
846 6. doi: 10.1002/2015GL063498.Received.
- 847 Struck, U. (2012) 'On The Use of Stable Nitrogen Isotopes in Present and Past Anoxic
848 Environments', in, pp. 497–513. doi: 10.1007/978-94-007-1896-8_26.
- 849 Swart, P., Evans, S. and Capo, T. (2008) *The Origin of Nitrogen Isotope Values in Algae*. Miami.
850 Available at:
851 [https://www.researchgate.net/publication/241642051_The_Origin_of_Nitrogen_Isotope_Values_i](https://www.researchgate.net/publication/241642051_The_Origin_of_Nitrogen_Isotope_Values_in_Algae)
852 [n_Algae](https://www.researchgate.net/publication/241642051_The_Origin_of_Nitrogen_Isotope_Values_in_Algae) (Accessed: 18 September 2019).
- 853 Tank, S. E. *et al.* (2012) 'The Processing and Impact of Dissolved Riverine Nitrogen in the Arctic
854 Ocean', *Estuaries and Coasts*. Springer-Verlag, 35(2), pp. 401–415. doi: 10.1007/s12237-011-
855 9417-3.
- 856 Thibodeau, B. *et al.* (2013) 'Heterogeneous dissolved organic nitrogen supply over a coral reef:
857 first evidence from nitrogen stable isotope ratios', *Coral Reefs*. Springer Berlin Heidelberg, 32(4),
858 pp. 1103–1110. doi: 10.1007/s00338-013-1070-9.
- 859 Thibodeau, B., Bauch, D. and Voss, M. (2017) 'Nitrogen dynamic in Eurasian coastal Arctic



- 860 ecosystem: Insight from nitrogen isotope', *Global Biogeochemical Cycles*, 31(5), pp. 836–849. doi:
861 10.1002/2016GB005593.
- 862 Tye, A. M. and Heaton, T. H. E. (2007) 'Chemical and isotopic characteristics of weathering and
863 nitrogen release in non-glacial drainage waters on Arctic tundra', *Geochimica et Cosmochimica*
864 *Acta*, 71(17), pp. 4188–4205. doi: 10.1016/j.gca.2007.06.040.
- 865 UNFCCC (2015) *Adoption of the Paris Agreement*. Available at:
866 <https://unfccc.int/resource/docs/2015/cop21/eng/l09r01.pdf> (Accessed: 2 September 2019).
- 867 Vasil'chuk, Y. K. *et al.* (2001) 'Radiocarbon Dating of $\delta^{18}\text{O}$ - δD Plots in Late Pleistocene Ice-
868 Wedges of the Duvanny Yar (Lower Kolyma River, Northern Yakutia)', *Radiocarbon*, 43(2B), pp.
869 541–553. doi: 10.1017/S0033822200041199.
- 870 Voigt, C. *et al.* (2017) 'Increased nitrous oxide emissions from Arctic peatlands after permafrost
871 thaw', *Proceedings of the National Academy of Sciences*, 114(24), pp. 6238–6243. doi:
872 10.1073/pnas.1702902114.
- 873 Vonk, J. E. *et al.* (2012) 'Activation of old carbon by erosion of coastal and subsea permafrost in
874 Arctic Siberia', *Nature*. Nature Publishing Group, 489(7414), pp. 137–140. doi:
875 10.1038/nature11392.
- 876 Vonk, J E *et al.* (2013) 'Dissolved organic carbon loss from Yedoma permafrost amplified by ice
877 wedge thaw', *Environmental Research Letters*. IOP Publishing, 8(3), p. 035023. doi:
878 10.1088/1748-9326/8/3/035023.
- 879 Vonk, J. E. *et al.* (2013) 'Dissolved organic carbon loss from Yedoma permafrost amplified by ice
880 wedge thaw', *Environmental Research Letters*, 8(3). doi: 10.1088/1748-9326/8/3/035023.
- 881 Vonk, Jorien E. *et al.* (2013) 'High biolability of ancient permafrost carbon upon thaw',
882 *Geophysical Research Letters*, 40(11), pp. 2689–2693. doi: 10.1002/grl.50348.
- 883 Walvoord, M. A. and Striegl, R. G. (2007) 'Increased groundwater to stream discharge from
884 permafrost thawing in the Yukon River basin: Potential impacts on lateral export of carbon and
885 nitrogen', *Geophysical Research Letters*. John Wiley & Sons, Ltd, 34(12), p. L12402. doi:
886 10.1029/2007GL030216.
- 887 Wankel, S. D. *et al.* (2007) 'Nitrification in the euphotic zone as evidenced by nitrate dual isotopic
888 composition: Observations from Monterey Bay, California', *Global Biogeochemical Cycles*, 21(2),
889 p. n/a-n/a. doi: 10.1029/2006GB002723.
- 890 Weigand, M. A. *et al.* (2016) 'Updates to instrumentation and protocols for isotopic analysis of
891 nitrate by the denitrifier method', *Rapid Communications in Mass Spectrometry*. John Wiley &
892 Sons, Ltd, 30(12), pp. 1365–1383. doi: 10.1002/rcm.7570.
- 893 Wild, B. *et al.* (2019) 'Rivers across the Siberian Arctic unearth the patterns of carbon release from
894 thawing permafrost.', *Proceedings of the National Academy of Sciences of the United States of*
895 *America*. National Academy of Sciences, 116(21), pp. 10280–10285. doi:
896 10.1073/pnas.1811797116.
- 897 Yi, Y. *et al.* (2012) 'Isotopic signals (^{18}O , ^2H , ^3H) of six major rivers draining the pan-Arctic
898 watershed', *Global Biogeochemical Cycles*. John Wiley & Sons, Ltd, 26(1), p. n/a-n/a. doi:
899 10.1029/2011GB004159.
- 900 Zhang, T. *et al.* (1999) 'Statistics and characteristics of permafrost and ground-ice distribution in
901 the Northern Hemisphere ¹', *Polar Geography*. Taylor & Francis Group, 23(2), pp. 132–154. doi:
902 10.1080/10889379909377670.



903 Zhang, T. *et al.* (2005) 'Spatial and temporal variability in active layer thickness over the Russian
904 Arctic drainage basin', *Journal of Geophysical Research*. John Wiley & Sons, Ltd, 110(D16), p.
905 D16101. doi: 10.1029/2004JD005642.
906